

Quantum Monte Carlo Studies of Electron–Electron Interaction Effects in Conducting Polymers

D. K. Campbell,¹ T. A. DeGrand,² and S. Mazumdar^{1,3}

We discuss recent studies, using the quantum ensemble projector Monte Carlo (EPMC) method, of theoretical models of conducting polymers. Our focus is on the consequences of incorporating direct electron–electron interactions into the “standard” electron–phonon interaction models. Among the observables we examine one energetics of purely dimerized ground states, single solitons, soliton pairs, averaged spin and charge distributions, and local correlation functions.

KEY WORDS: Quantum Monte Carlo; solitons; polyacetylene; Peierls–Hubbard models; quasi-one-dimensional systems.

The most important impetus driving the current explosion of effort on quantum Monte Carlo methods is their ability to provide quantitative answers, *and* physical insight, to problems where more conventional methods (e.g., perturbation theory, or Hartree–Fock and similar effective single-particle theories) fail. One class of such problems involves strongly interacting electron systems in condensed matter physics where an accurate treatment of true many-body effects is absolutely essential. In this article, we discuss one specific class of real materials in which these electron–electron interaction effects may play a significant role: namely, quasi-one-dimensional conducting polymers. Although relatively “simple” on the scale of some of the systems (e.g., lattice gauge theories) studied in other contributions to these proceedings, conducting polymers—and other synthetic metals such as charge transfer salts—have attracted enormous theoretical and experimental interest in recent years. In part this interest arises from

¹ Center for Nonlinear Studies, Los Alamos National Laboratory, Los Alamos, New Mexico 87545 U.S.A.

² Department of Physics, University of Colorado, Boulder, Colorado 80309 U.S.A.

³ Present address: GTE Laboratories, 40 Sylvan Rd., Waltham, Massachusetts 02254 U.S.A.

the many "exotic" broken symmetry ground states—charge and spin density waves (CDW, SDW), bond order waves (BOW), and singlet and triplet superconductivity (SSC, TSC)—that are theoretically possible in quasi-one-dimensional systems. Moreover, the technological potential of "plastics that conduct"—and maybe even *superconduct*—has not detracted from this interest. For additional background and up-to-date surveys of this broader field of synthetic metals, interested readers are referred to recent conference proceedings^(1,2) and reviews.⁽³⁾

To be concrete, we focus entirely on one specific conducting polymer: *trans*-polyacetylene (henceforth, $(\text{CH})_x$). In the theoretical idealization, this polymer is an infinite chain, with individual (CH) units connected in the

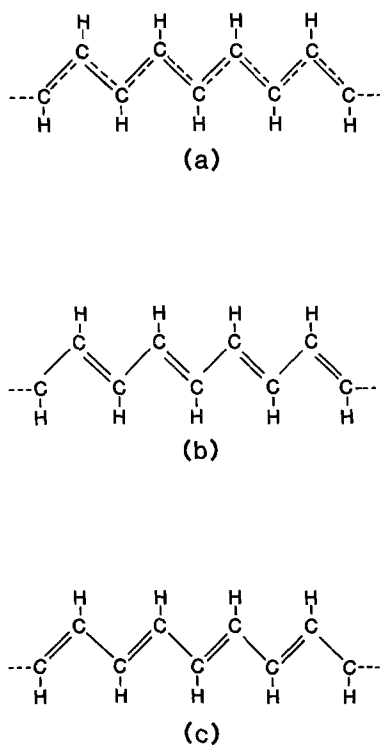


Fig. 1. (a) A (hypothetical) infinite *trans*- $(\text{CH})_x$ chain with uniform bond lengths, that is, no dimerization; (b) and (c) The two-degenerate bond alternation patterns of the actual *trans*- $(\text{CH})_x$ polymer. The CH units linked by double bonds are slightly closer ($\cong 0.10 \text{ \AA}$) together than those linked by single bonds. The degeneracy in energy between these two structures is essential for the presence of kink soliton excitations.

herringbone fashion shown in Fig. 1. Since $(\text{CH})_x$ may be unfamiliar to many readers, we begin with a (minimal) introduction to the current theoretical approaches to this material.

The (apparent) chemical simplicity of $(\text{CH})_x$ has made it a central focus of research by both chemists and physicists interested in conducting polymers. In general, theorists in both groups agree that a model involving only the electrons in the π -molecular orbital should be a reasonable first approximation. Since this π orbital is composed essentially of carbon atomic p orbitals, each containing one electron, both the chemists' and the physicists' models correspond to half-filled (one electron/site) one-dimensional chains. Beyond this point, however, the dogmas of the two groups have diverged.

Physicists, following Peierls, have focused on the electron–phonon interaction describing the effects of the π electrons on the backbone lattice of (CH) units. The experimentally observed dimerization/bond alternation⁽⁴⁾—that is, the fact that the (CH) units linked by double bonds in Fig. 1 are physically closer to each other than those linked by single bonds—confirms the importance of this interaction. Clearly this bond alternation breaks the symmetry of the uniformly spaced (undimerized) chain; in the terminology mentioned above, this broken symmetry state is called a bond order wave (BOW). In the context of *trans*- $(\text{CH})_x$, the specific Peierls-like model developed by Su, Schrieffer, and Heeger (SSH)⁽⁵⁾ has stimulated considerable interest, particularly because of its prediction that nonlinear ‘soliton’ excitations—‘kinks’ (with exotic spin/charge relations), polarons, and ‘breathers’—would play an important role in the observable properties of the polymer. Since the electrons interact directly only with the phonons and not with each other, the SSH model is a single-electron theory. Consequently, it can readily be studied both numerically⁽⁵⁾—in the discrete, lattice version, even for (adiabatic) dynamics—and, in the continuum limit, analytically.⁽³⁾ The original SSH model, however, takes no explicit account of the direct interactions between the electrons.

In contrast, chemists have asserted that direct electron–electron interactions—essentially Coulombic repulsions, either long-range or screened—are the dominant feature of quasi-one-dimensional conducting polymers. Their theorists have used various techniques to study models, such as the Pariser–Parr–Pople (PPP) Hamiltonians incorporating these effects. For an introduction to this class of models to finite polymers see Ref. 6. Since these models involve explicit electron–electron interactions, they lead invariably to many-electron problems. A terminology common in the literature, and one we adopt, is to refer to these interacting many-electron systems as “correlated bands” and to use the term “correlation effects” when we mean the effects of direct electron–electron interactions. Many

electron problems are generally analytically inaccessible, except by approximate methods such as Hartree-Fock. Unfortunately, it has recently become clear⁽⁷⁾ that, precisely in models of quasi-one-dimensional conducting polymers, these approximate methods can lead to *qualitatively incorrect results*. Further, correlated band problems are also numerically daunting, since the number of electron states grows roughly as 4^N , where N is the number of lattice sites. Thus *exact* diagonalizations of PPP Hamiltonians for finite-size systems can at present be carried out only up to $N \cong 12$.⁽¹⁰⁾

As an (important) illustration of the differences between the two types of models, consider the interpretation of the experimental data on optical absorption in *trans*-(CH)_x. In the physicists' electron-phonon models, the optical gap is attributed entirely to the change in the Fermi surface caused by the "Peierls distortion" that leads to the dimerization of the chain. In the chemists' models, on the other hand, the optical gap comes at least in part from the electron-electron interactions—as is familiar from the exact solution⁽¹¹⁾ to the half-filled Hubbard model—and there would be a gap even if there were no dimerization of the chain.

In view of the considerably greater simplicity of the single-electron models, it is natural to hope that some variant of the SSH model—with effective parameters chosen to include some of the electron-electron interaction effects and perhaps with a perturbative treatment of additional direct interactions—would apply to (CH)_x. Unfortunately, three clear pieces of experimental data strongly suggest that this is not the case. First, the observed ordering of the excited states⁽¹²⁾ in finite polyenes—for example, octatetraene, which has 8 CH units—is inconsistent with *any* (one-dimensional) single-electron model but can be well-described by models incorporating correlations. Second, the observation (via coupled electron-nuclear magnetic resonance⁽¹³⁾) of negative spin densities on alternate carbon atoms is inconsistent with a pure SSH model no matter how the parameters are chosen. Third, the optical absorption from neutral kink solitons occurs near the "band edge,"⁽¹⁴⁾ rather than at midgap, as predicted by the SSH model. This indicates that correlation effects are playing an important—and not just a perturbative—role in the observed optical properties of *trans*-(CH)_x. All in all, an objective view of the full experimental situation requires that one adopt neither the chemists' nor the physicists' dogma but instead study, nonperturbatively and without using Hartree-Fock techniques, models involving both electron-phonon and electron-electron interactions. In the remainder of this contribution, we summarize some of the results of several recent studies along these lines.^(9,15,16) The Hamiltonians that have been studied belong to a class that can be termed 'Peierls-Hubbard' models

$$\begin{aligned}
H = & (1/2M) \sum_i p_i^2 + (K/2) \sum_i (y_i - y_{i+1})^2 \\
& + \sum_{i,s} [t_0 - \alpha(y_i - y_{i+1})] (c_{i,s}^+ c_{i+1,s} + \text{h.c.}) \\
& + (U/2) \sum_{i,s} \rho_{i,s} \rho_{i,-s} + V_1 \sum_i \rho_i \rho_{i+1} + \sum_{j \geq 2} \sum_i V_{i+j} \rho_i \rho_{i+j} \quad (1)
\end{aligned}$$

Here y_i and p_i represent (respectively) the displacement and momentum of the i th (CH) unit and thus describe the *intersite* phonons of the backbone lattice. One can also consider models for systems in which the individual chemical units are themselves complicated molecules having localized *intrasite* phonons coupled to the onsite charge density. Charge transfer solids provide a physical example of such systems. For simplicity and in view of our interest in $(\text{CH})_x$ we ignore these additional terms here. The operator $c_{i,s}(c_{i,s}^+)$ annihilates (creates) an electron of spin $s(= +\frac{1}{2}, -\frac{1}{2})$ at site i . The electron density is $\rho_{i,s} = c_{i,s}^+ c_{i,s}$ and $\rho_i = \rho_{i,s} + \rho_{i,-s}$. The first two lines of (1) are just the conventional SSH model, with parameters M (the (CH) unit mass), K (representing the strain energy of the σ bonds), t_0 (the bare hopping), and α (the electron-phonon coupling). The third line contains the standard extended Hubbard interactions: an on-site repulsion $U(>0)$ and a (repulsive) nearest-neighbor interaction ($V_1 > 0$). The final line represents long-range electron–electron interactions via the parameters V_j for $j > 2$. Clearly, (1) contains the usual SSH, Hubbard, and extended Hubbard models, and for specific choices of U and the V_j can reproduce any of the parameterizations of the PPP model.^(6,9,16)

In view of our focus on quantum Monte Carlo methods, we treat only the extended Hubbard model: that is, the first two lines of (1). Although there are some results^(10,16) on the effects of long-range interactions (V_j , with $j \geq 2$), they have not been obtained with Monte Carlo techniques.

Our studies neglect the dynamical (quantum) nature of the phonons: formally, this amounts to taking $M \rightarrow \infty$ —the Born–Oppenheimer limit—in (1). In fact, careful analysis⁽¹⁷⁾ of the effects of quantum phonons indicate that—as one might expect in view of the large (CH) mass—for most properties this neglect provides a *quantitatively* good approximation. To investigate the extended Hubbard model ($U, V_1 \neq 0$) we use the recently developed the “ensemble projector Monte Carlo” technique.^(9,15,18) Stripped of technical details, the EPMC method is based on the observation that for an arbitrary wave function Ψ and for large β

$$\exp(-\beta H) \Psi = \exp(-\beta E_0) \{c_0 \Phi_0 + 0[\exp - \beta(E_1 - E_0)]\} \quad (2)$$

where Φ_0 is the true ground state. In words, (2) says that applying the operator $\exp(-\beta H)$ for large β “projects out” the ground state (Φ_0) with

exponential accuracy (assuming there is a gap, that is, that $E_1 - E_0 \neq 0$) provided only that the chosen trial function is *not* orthogonal to Φ_0 (that is, $c_0 \neq 0$). In practice, we take Ψ to be an ensemble (typically with 5000 members) of real space configurations. Hence the name EPMC. Details of the method are available elsewhere.^(9,18)

In our experience, the EPMC gives very accurate energies even for relatively large ($N \cong 30$) systems, gives acceptable spatially averaged quantities—for example, the overall ratio of negative to positive spins—but gives fairly poor local information on the wave function unless an unacceptably large number of states is used in the ensemble. To illustrate these comments, we give below results for each of these three types of observables.

From energetic studies alone we can learn much about the influence of electron–electron interactions. A natural first question is: “Does the dimerization found in the SSH model persist in the presence of strong e – e interactions?” This is of great interest for two reasons. First, the broken symmetry and two-fold degenerate ground state corresponding to the dimerization are essential for the presence of kink solitons. Second, based on earlier results obtained by approximate methods, it was believed that

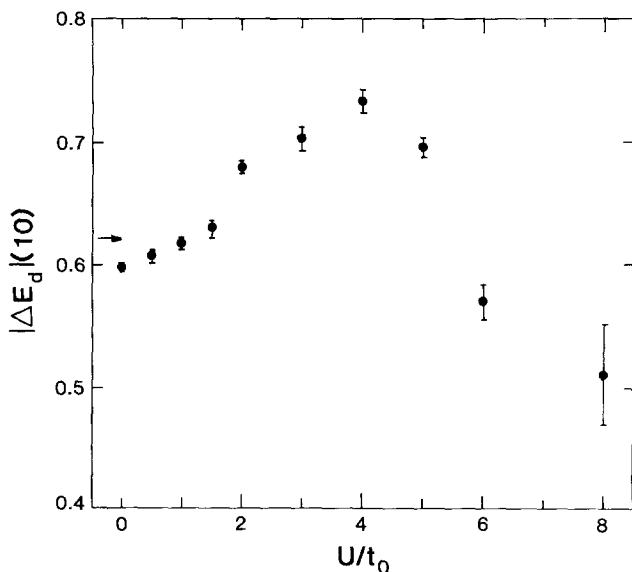


Fig. 2. The magnitude of the electronic energy difference between a dimerized $(\text{CH})_x$ chain with $\delta = 0.1$ (see text) and a uniform chain for an $N = 32$ site ring plotted vs the onsite Hubbard parameter U . The arrow on the left indicates the exact $U = 0$ result. The enhancement of the energy gained upon dimerization for intermediate U is clearly shown.

even moderate correlations would destroy dimerization. For a thorough discussion of the Hartree–Fock results for the extended Hubbard model as applied to polyacetylene see Ref. 19. Since dimerization has been observed in $(\text{CH})_x$, this (incorrect) belief was used to assert that the e – e interactions had to be small. In fact, our results confirm earlier recent studies (using both Monte Carlo⁽⁷⁾ and exact diagonalization methods⁽⁸⁾) that even fairly strong on-site interactions— $U \cong 4t_0$ —actually *enhance* dimerization. The inclusion of V_1 (up to $V_1 = \frac{1}{2}U$, see below and Ref. 16) tends to enhance dimerization further. This is shown in Fig. 2, where the (electronic) energy gained upon dimerization is plotted versus U for $V_1 = 0$. Note that ΔE_d is defined as the difference between a system in which the sequential transfer integrals alternate between $t_{i,i+1} = t_+ = t_0(1 + 2\delta)$ and $t_{i,i+1} = t_- = t_0(1 - 2\delta)$ and the uniform system with all $t_i = t_0$. The data in Fig. 2⁽⁹⁾ are for a $N = 32$ site (closed) ring with $\delta = 0.1$ and show clearly the tendency of U to enhance the dimerization.

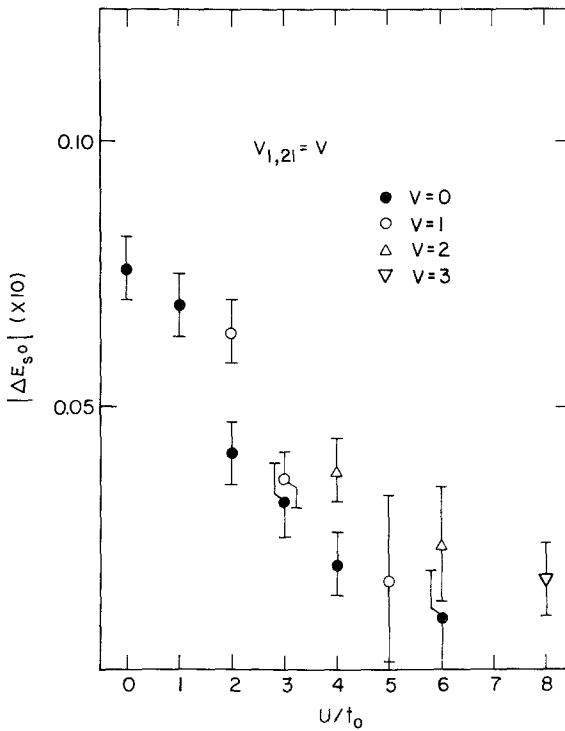


Fig. 3. The magnitude of the persite electronic energy difference between the neutral soliton and the neutral dimer for $N = 21$ plotted versus U for several values of $V_1 = V$. The soliton is always lower in energy.

Since the EPMC method appears to yield information only about ground states, one might wonder how we are able to extract information about kink solitons, which one normally thinks of as excited states of the polymer. In fact, for finite odd (open) chains, it has been known for some time⁽²⁰⁾ that the ground state in the SSH model—that is, for U and $V_j = 0$ —is a kink soliton, rather than a pure dimer. Does this situation persist in the presence of correlations? In Figs. 3 and 4 we show the results for both the neutral (Fig. 3) and charged (Fig. 4) solitons for a $N=21$ unit chain with $\delta=0.1$. Note that in our EPMC approach, a soliton in the backbone chain is *defined* as a reversal of the bond alternation pattern about a *single* site. This single-site soliton is clearly not optimal variationally—one would expect the lattice to relax over several sites—but nonetheless one sees from the figures that the solitons remain the ground states even at large U and V_1 . Note the clear difference between the case of the neutral soliton—where the energy difference falls continuously with U

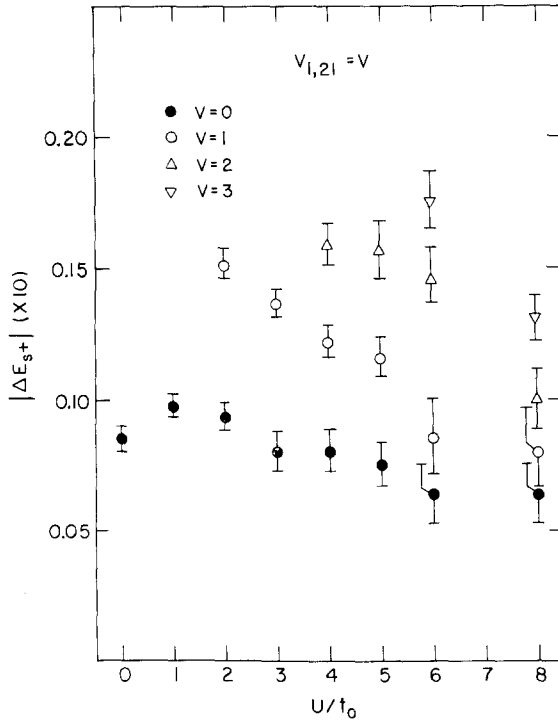


Fig. 4. The magnitude of the persite electronic energy difference between the positively charged soliton and the positively charged dimer for $N=21$ plotted versus U for several values of $V_1 = V$. The soliton is always lower in energy.

and V_1 and is, within numerical uncertainties, a function of $U - V_1$ only—and that of the charged soliton, where there is an initial *increase* in the energy difference before a much slower decrease and where nonzero V_1 greatly increases the stability of the soliton vis-a-vis the dimer. Several further points should be made. First, within errors, $\Delta E_{S^+} = \Delta E_{S^-}$, as one would expect from the particle-hole symmetry of (1) in the half-filled band. Second, the trends in the energy differences for $U \cong 0$ are consistent with perturbation theory results.⁽²¹⁾ Third, the curves in the figures are all for $V_1 < \frac{1}{2}U$; this is necessary for the ground state of (1) to remain a BOW. For $V_1 > \frac{1}{2}U$, the ground state becomes an on-site charge density wave (CDW).⁽¹⁶⁾ Finally, the presence of a nearest-neighbor term ($V_{1,21} = V_1$) between the two ends of the open chain is a technicality necessary to preserve the correct symmetries of the Hamiltonian in the finite-chain case.^(9,15)

The last point we study with energetics is the experimentally crucial issue of soliton doping: does a system of $N - 2$ electrons (for p -type doping) on N sites prefer to have two solitons (S^+, S^+), or to be a doubly charged dimer (D^{2+})? In Fig. 5 we present our data indicating that, at least for $U < 6t_0$, the S^+S^+ configuration is lower in energy than the D^{2+} . Thus soliton doping persists even for relatively strong correlations.

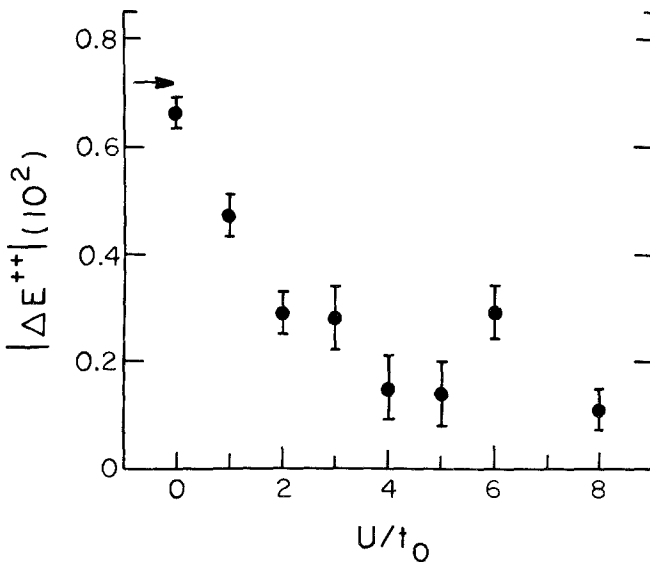


Fig. 5. The magnitude of the difference between the S^+S^+ and the D^{2+} configurations (see text) on a $N = 18$ unit chain. The S^+S^+ configuration is always lower in energy, indicating that ‘soliton doping’ persists for $U = 0$. The arrow marks the exact energy difference for $U = 0$.

To illustrate the nature of our EPMC results for spatially averaged correlation functions we plot in Fig. 6 the ratio of the sum of the excess negative spin ($\rho_- < 0$) to the excess positive spin ($\rho_+ > 0$) for a nine-site chain containing a neutral soliton. Since the neutral soliton has a total of 1 unit of net spin, $\rho_+ + \rho_- = 1$. For the spin-up soliton in the SSH model, $\rho_- = 0$. When correlations are present, $\rho_- \neq 0$ and the ratio can take on a nonzero value. Although the data are sparse, within errors this ratio appears to be a function of $U - V_1$ alone. The point labeled PPP is the result of an exact finite-size diagonalization of the PPP model with certain specific V_j ; ⁽¹⁰⁾ it is also the value deduced from experiment. ⁽¹³⁾ Note the (modest) dependence on the number of states in the ensemble and the deviation, at $U = 0 = V_1$, from the known exact answer ($\rho_- / \rho_+ = 0$).

As a final illustration of the EPMC method, we show in Fig. 7 the site-by-site spin and charge distributions of neutral and charged solitons (respectively) for a $N = 9$ site chain. The solid curve represents the exact

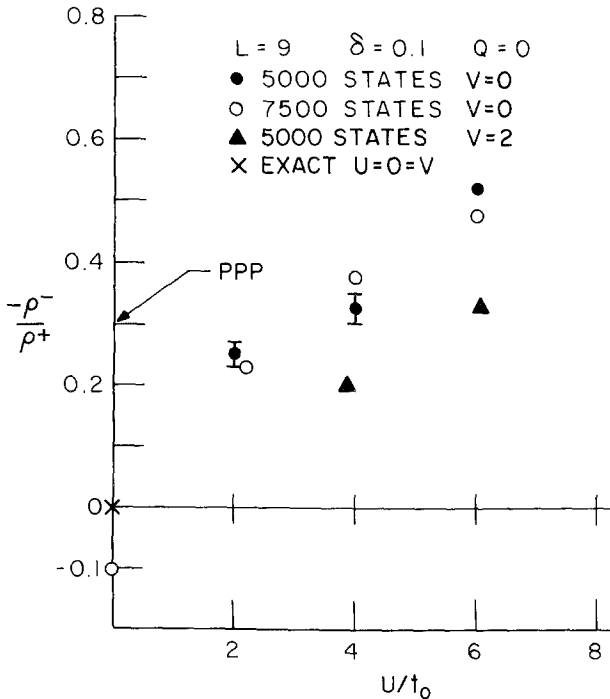


Fig. 6. The ratio of the sum over a 9-site chain of the excess negative spin to the sum of the excess positive spin for a neutral soliton. Since the neutral soliton has a total of one unit of spin, $\rho_+ + \rho_- = 1$. For the SSH model, $\rho_- = 0$ and $\rho_+ = 1$. When correlations are present, $\rho_- \neq 0$.

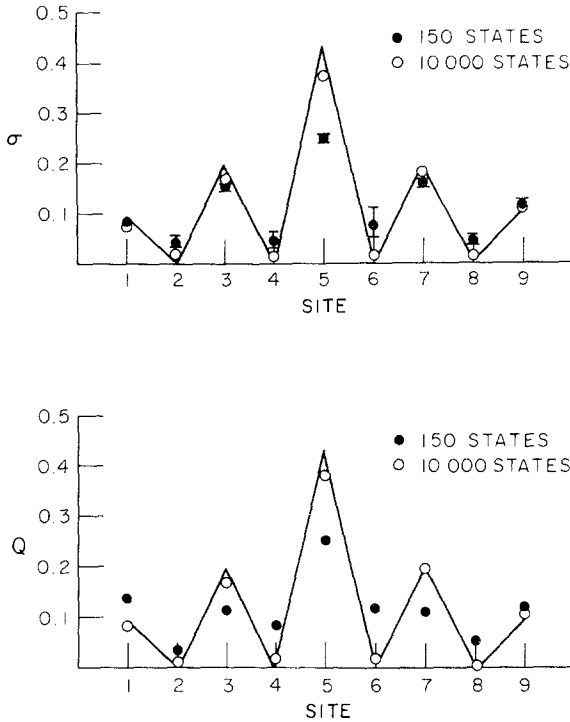


Fig. 7. The spin (σ) and charge (Q) distributions for neutral and charged (respectively) solitons on a $N=9$ site chain. The solid lines are the exact SSH results and the data points are EPMC results for two different size ensembles.

result for $U=V=0$, while the two sets of data points represent results of EPMC runs with different size ensembles. For 150 states, the EPMC results show strong systematic errors. Although the 10,000 state ensemble does reproduce the exact answer (within errors) for this $N=9$ case, since the number of states needed in the EPMC ensemble is expected to grow rapidly with system size, we see that, unless improvements can be made in the sampling procedure, obtaining accurate information on the detailed wave functions for any reasonable size system would require using unacceptably large ensembles.

In summary, we have shown that quantum Monte Carlo techniques can provide essential insight into the physics of quasi-one-dimensional conducting polymers when electron–electron interactions are added to the standard electron–phonon models. Although much progress has been made, many questions—for example, the nature of the optical gap, optical absorption, and photo-induced absorption—remain unanswered when both types of interactions are present. Further, as the number of interesting

new real quasi-one-dimensional materials^(1,2)—conducting polymers, charge transfer solids, blue bronzes—continues to grow, the possibilities for clear experimental confirmation (or refutation!) of theoretical predictions increase. Thus the subject of low-dimensional real materials remains one of the most exciting areas to which quantum Monte Carlo methods can be applied.

ACKNOWLEDGMENTS

This work was supported in part by the United States Department of Energy. One of us (D.K.C.) thanks M. Peyrard and M. Remoisenet of the Lab. d'Optique du Réseau Cristallin at the Université de Dijon for hospitality while some of the manuscript was written.

REFERENCES

1. Proceedings of the International Conference on Synthetic Metals (ICSM 84), Abano Terme, Italy, June 1984, *Mol. Cryst. Liq. Cryst.* **118** (1985).
2. Proceedings of Synmetals III, Third Los Alamos Conference on Synthetic Metals, April 1985, to be published in *Synthetic Metals*.
3. T. Skotheim, ed. *The Handbook of Conducting Polymers* (Marcel Dekker, New York, 1985).
4. C. Fincher et al., *Phys. Rev. Lett.* **48**:100 (1982); C. S. Yannoni and T. C. Clarke, *Phys. Rev. Lett.* **51**:1191 (1983).
5. W. P. Su, J. R. Schrieffer, and A. J. Heeger, *Phys. Rev. Lett.* **42**:1698 (1979); *Phys. Rev. B* **22**:2099 (1980).
6. L. Ohmine, M. Karpplus, and K. Schulten, *J. Chem. Phys.* **68**:2298 (1973).
7. J. Hirsch and M. Grabowski, *Phys. Rev. Lett.* **51**:1713 (1984).
8. S. Mazumdar and S. N. Dixit, *Phys. Rev. Lett.* **51**:292 (1983); *Phys. Rev. B* **29**:1824 (1984).
9. D. K. Campbell, T. A. DeGrand, and S. Mazumdar, *Phys. Rev. Lett.* **52**:1717 (1984) and *Phys. Rev. B* (to be submitted), and references therein.
10. Z. G. Soos and S. Ramasesha, *Phys. Rev. Lett.* **51**:2374 (1983); *Phys. Rev. B* **29**:5410 (1984).
11. E. Lieb and F. Y. Wu, *Phys. Rev. Lett.* **20**:1445 (1968).
12. B. S. Hudson et al., in *Excited States*, E. C. Lim, ed. (Academic, New York, 1982).
13. H. Thomann, L. R. Dalton, Y. Tomkiewicz, N. S. Shiren, and T. C. Clarke, *Phys. Rev. Lett.* **50**:533 (1983).
14. B. R. Weinberger, C. B. Roxlo, S. Etemad, G. L. Baker, and J. Orenstein, *Phys. Rev. Lett.* **53**:86 (1984).
15. D. K. Campbell, T. A. DeGrand, and S. Mazumdar, *Mol. Cryst. Liq. Cryst.* **118**:41 (1985).
16. S. Mazumdar and D. K. Campbell, *Phys. Rev. Lett.* **55**:2067 (1985), and references therein.
17. J. E. Hirsch and E. Fradkin, *Phys. Rev. Lett.* **49**:402 (1982); *Phys. Rev. B* **27**: 1680 and 4302 (1983).
18. R. Blankenbecler and R. L. Sugar, *Phys. Rev. D* **27**:1307 (1983).
19. K. R. Subbaswamy and M. Grabowski, *Phys. Rev. B* **24**:2168 (1981).
20. W. P. Su, *Solid State Commun.* **35**:899 (1980).
21. S. Kivelson and D. E. Heim, *Phys. Rev. B* **26**:4278 (1982).